Preliminary mission analysis and design of ISTsat-2

Bruno Emanuel Fernandes Leal Duarte Pacheco
bruno.pacheco@tecnico.ulisboa.pt

Instituto Superior Técnico, Universidade de Lisboa, Portugal

November 2021

Abstract

ISTsat-2 is the second satellite project of Instituto Superior Técnico. ISTNanosat team is responsible for its development, which aims to provide students hands-on experience in the aerospace industry. In this work the preliminary analysis and design of a mission proposal for ISTsat-2 is done. The use of two CubeSats, 2U ($10\times10\times20$ cm^3) and 1U ($10\times10\times10$ cm^3) form factor, launched together as a 3U and separated in orbit is proposed. The main objectives are ground observation and control of the relative distance between the satellites. The remote sensing goal is the detection of vessels through images and subsequent comparison with Automatic Identification System (AIS) data. From the objectives and requirements the basic aspects of satellite behavior in orbit, such as lifetime, visibility and eclipse, are analyzed. Lastly, a preliminary satellite design and an analysis of the power and mass budget, based on a selection of Commercially Off-The-Shelf (COTS) products, are presented.
Keywords: mission analysis, Earth observation, CubeSat, relative distance, preliminary design

1. Introduction

In 1957 the world witnessed the launch of Sputnik 1 (a sphere with 58.5 cm in diameter and 83.6 kg [1]), the Earth's first artificial satellite. This event marks the beginning of the well-known Space Race. In 1969 the United States of America wins the race with the arrival of man to the Moon. By this time the economic exploitation of the satellites was controlled by the government. The construction of a satellite required advanced technical resources and high funding, in addition to the cost and complexity of launches [2].

Space became more accessible with electronic miniaturization, which allowed a significant reduction of satellite dimensions. The use of Commercial Off-The-Shelf (COTS) products has allowed the creation of small satellites at a fraction of mass, cost and time. In this paper the preliminary mission planning of a small satellite is developed. The main goal is the mission definition, analysis and design of the system.

2. Mission definition

In this section mission objetives and requirements are defined. Finally, a brief description of the mission and the satellites is given.

2.1. Mission objectives

The primary goal of this and similar university projects is always educational, i.e., to allow participants hands-on experience working on space projects where success is measured by the learning acquired during the development phase. The mission aims to study the control and maintenance of the relative distance between two CubeSats in Low Earth Orbit (LEO). Maintaining this distance will also allow testing inter-satellite communications. The use of two satellites allows maximizing the mission's coverage area. As a way to support in monitoring and controlling the Portuguese maritime territory a remote sensing system will be used as payload for ship detection. The mission thus contemplates three main objectives: distance control between the satellites, inter-satellite communication and Earth observation, more specifically of the ocean.

Once the mission's objectives have been defined, it is possible to determine some requirements that derive from them. The requirements may suffer updates during the project's evolution process, normally used as preliminary assumptions. For distance control and inter-satellite communications, a highly accurate attitude determination and control system is needed. Since this is a university project the proposed ground resolution is to be as high as possible taking into account the size and limitations of the CubeSat format considered. Taking into account that the mission is based on two CubeSats there are also requirements imposed on the construction of this specific type of satellite in order to respect the limits of mass and dimensions. Daily communication with the ground station is also con-

sidered a requirement of the mission.

2.2. Relative distance control using differential drag

Aerodynamic resistance is an opposing force to the motion of an object created by the atmosphere surrounding it.

The value of this force is directly related to the density of the atmosphere, which decreases with altitude. In the upper layers of the atmosphere the density value is reduced, but over time the atmospheric friction causes an energy dissipation of the system and subsequently the decay of the orbit (reduction in altitude) and eventual reentry. Aerodynamic drag plays a dominant role in the major disturbances acting on a satellite, especially in LEO.

The acceleration due to drag can be expressed using the equation (1), where ρ is the atmospheric density, C_D is the drag coefficient, A is the section area of the satellite perpendicular to the motion, m is the mass of the satellite, and v is the velocity.

$$a_D = \frac{1}{2}\rho C_D \frac{A}{m} v^2 \tag{1}$$

Aerodynamic drag is strongly affected by local variations in atmospheric density, especially at lower altitude. The variations are mainly caused by solar influence [3]. From the equation it can be stated that if two satellites are passing through layers of the atmosphere with similar density (equal ρ) the difference in drag acceleration depends only on the physical characteristics of the satellites, which can be expressed as the ballistic coefficient (equation (2)).

$$BC = \frac{m}{C_D A} \tag{2}$$

If no control mechanism is applied, the aerodynamic resistance in addition to other disturbances eventually causes the satellites to drift apart.

However, it is possible to use the satellites characteristics (area and mass) to purposely create an aerodynamic resistance differential by changing the value of the ballistic coefficient. This differential can be used to control the position of one satellite relative to others. In 1986 it was proposed the maintenance of a satellite formation using aerodynamic resistance [4].

Changing the mass is usually irreversible and only possible when propellant is used, which is not common in the CubeSat domain. However, there are ways to adjust the value of the drag area. In [5] plates are used that when adjusted the direction relative to the velocity create more or less drag area. These plates can also be used as solar panels [6].

A second option is to take advantage of the asymmetry of one of the satellites and rotate it about itself in order to create a larger area. An increase in area causes a decrease in the ballistic coefficient. One can conclude from the equations (1) and (2) that this decrease causes an increase in the aerodynamic drag acceleration (absolute value).

2.3. Vessel identification

Given its geographical position, Portugal has always been connected to the sea. The maritime areas under national jurisdiction, which include among others the Exclusive Economic Zone (EEZ) and the Continental Shelf, cover about four million km^2, making Portugal the largest coastal state in the European Union.

In the control of maritime traffic, cargo and passenger transport, pollution, oil spills, illegal fishing, defense, piracy, etc., it is necessary to have the detection and identification of all vessels passing through the national maritime space.

One of the most important roles of coastal states, defined by the International Maritime Organization (IMO), is the safety of navigation, that is, the control of maritime traffic in order to avoid possible accidents. For this, and to assist crews on board ships and boats, there are control services (Vessel Traffic Service (VTS)) that in real time monitor all maritime traffic, particularly areas with high movement as ports. Typically the VTS systems employ radar, radio (VHF) and the Automatic Identification System (AIS) [7].

AIS is one of the most used for vessel tracking, the system constantly sends a ship's location to others and to the coastal authorities, created primarily to avoid collisions A large portion of small ships (less than 300 tons) and most fishing boats are not required to use AIS. For this reason the use of image or radar surveillance is an added value as a complement to AIS.

2.4. Mission description

The mission focuses on the development and construction of two CubeSats, satellite A (2U) and B (1U), launched together as a 3U. Once in orbit the satellites are separated by means of a mechanism, which may or may not induce a separation velocity.

The distance between the satellites is controlled by using the difference in aerodynamic resistance applied to each of them. The use of satellites with different sizes and masses enables a difference in ballistic coefficients that allows the relative distance between them to be controlled by varying the projected area of the larger satellite.

Satellite B has a simpler attitude control system, similar to the one used in ISTsat-1. In addition, it has an AIS as payload that allows obtaining data to identify ships.

Satellite A, with an active control system, is responsible for maintaining the distance between satellites by changing their position relative to ve-

locity. This satellite also has an optical sensor that provides the highest resolution possible in order to identify smaller vessels.

The data obtained by both satellites is then analyzed and compared in order to find vessels that are not properly identified.

3. Mission analysis

Mission analysis is the process of quantifying the system parameters and their results to ensure that the mission requirements are met.

The goal of this chapter is to analyze the influence of the orbit and the solutions found to meet the requirements on all aspects of the satellite's life, such as orbital decay, visibility, and eclipse. This process is iterative in order to study several possibilities and find the one that best fits the mission objectives and constraints. NASA's General Mission Analysis Tool was the software used to simulate the satellite's orbit.

3.1. Preliminary analysis

The mission is composed of two satellites: one 1U CubeSat and a 2U CubeSat, launched together and then separated in orbit by a separation mechanism. Assuming that this mechanism uses springs, this implies a velocity imposed on each satellite with opposite directions. Considering as initial orbit, the ISS orbit on January 1, 2021 at 12 h:41 min:12 s :

- Altitude, $h = 420\,\text{km}$
- Inclination, $i = 51.647°$
- Eccentricity , $e = 0,00011$
- Longitude of the ascending node, $\Omega = 116.098°$
- Argument of periapsis , $\omega = 176.5108°$
- True anomaly, $E = 62.1377°$
- Period, $T = 5569.4\,\text{s}$

It was considered that the separation is performed parallel to the orbit and conservation of linear momentum was taken into account. An initial simulation was performed using the data presented above. In the figure 1 it is possible to see the distance between the two satellites, measured in a straight line in three different situations: without separation mechanism and with separation mechanism but with two different velocities.

When the drag coefficient is $C_D = 2.2$ and separation velocity $v_s = 0\,\text{cm}$ we can see, in figure 1, that the distance between the satellites is only 4.2 km. However, although it is not visible on the graph due to the scale, on the fourth day of the simulation the line touches zero. This means that the satellites get closer and one passes by the other. To minimize the risk of collisions after launch a separation velocity will be applied. During this work the value of $v_s = 12\,\text{cm}\,\text{s}^{-1}$ will be used.

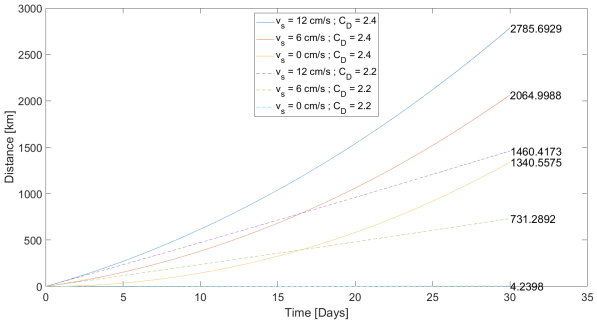

Figure 1: Comparison of the relative distance between satellites in three cases: without separation velocity, with velocity equal to $6\,\text{cm}\,\text{s}^{-1}$ and $12\,\text{cm}\,\text{s}^{-1}$ and for two values of air drag coefficient $C_D = 2.4$ and $C_D = 2.2$. The projected area is considered to be $0.02\,\text{m}^2$ and $0.01\,\text{m}^2$ for satellites A and B, respectively. The simulation was performed using GMAT.

The straight line distance, shown in figure 1, also represents the necessary range of the link for inter-satellite communications. This distance in turn is limited by system characteristics and mission requirements. From the point of view of small satellites, communication between them makes sense when the distances are not too long, since they are limited by the amount of energy they can produce and, as already mentioned, by their dimensions. In the literature, values for range in communication between small satellites vary between 10–25 km [8], 90 km [9] and even 1000 km [10].

This means that distances on the order of those shown in the figure 1 are too high and for this reason a solution needs to be applied to keep the satellites within a more favorable range for communication.

3.2. Relative distance control

As introduced, the distance between the satellites is a result of the difference between the ballistic coefficient of the two. It was also mentioned the use of the projected area to vary the value of the ballistic coefficient.

Since the goal is to maintain the distance between the satellites what is intended is to vary the projected area of CubeSat A which in turn varies the drag acceleration and consequently brings the satellites closer together or further apart. This solution thus presents two requirements to be taken into account: continuous ground observation and variation of the projected area of satellite A. To conjugate the two presented requirements the satellite could assume two positions: point a long or small face to nadir and in both cases rotate according to a yaw angle. In the first case the minimum projected area would be $0.01\,\text{m}^2$, while in the second case it would be double. That is, in the second case satellite A

would never have a lower ballistic coefficient than satellite B, for this reason reducing the distance between the two would not be possible.

The figure 2 shows the projected area of a 2U shaped CubeSat. Shown in the figure is the maximum area of approximately $0.03\,\mathrm{m}^2$, when $\alpha = 42°$ and $\psi = 63°$ and the minimum area of $0.01\,\mathrm{m}^2$ at the initial position.

The region called the area of interest (figure 2) represents the variation of the yaw angle, ψ, and the area projected by this variation in case the satellite has a long face pointing towards the Earth. Thus the maximum area obtained is approximately $0.022\,\mathrm{m}^2$ when $\alpha = 0°$ and $\psi = 63°$ and the minimum is $0.01\,\mathrm{m}^2$.

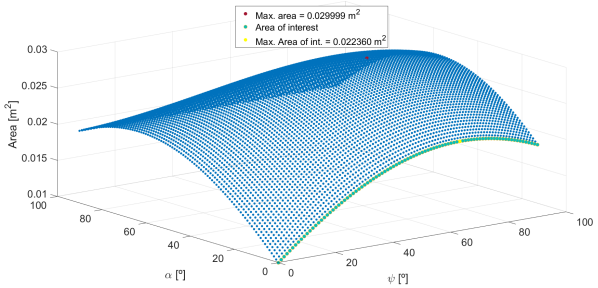

Figure 2: Projected area of a 2U form factor, where α and ψ are the pitch and yaw angles, respectively. The area of interest represents the area considered according to the given requirements.

Next, the range of the area of interest was used to study the variation of the ballistic coefficient of both satellites, figure 3. Considering that satellite B maintains its attitude and therefore a projected area of $0.01\,\mathrm{m}^2$, it is identified that for the satellites to equal the ballistic coefficient it is necessary that satellite A has a projected area of approximately $0.018\,\mathrm{m}^2$ (called $\mathrm{Area_n}$) in the case of $C_D = 2.4$ and $0.02\,\mathrm{m}^2$ for $C_D = 2.2$. These values correspond to $\alpha = 0°$ and $\psi = 28°$ and $\alpha = 0°$ and $\psi = 90°$.

When the ballistic coefficients area equal the distance between the satellites increases uniformly, because the acceleration caused by aerodynamic resistance is equal in both satellites.

When the ballistic coefficient of the 2U satellite is greater than the 1U (above the horizontal straight line passing through the yellow and green points in the figure 3) the satellites move apart at first but come closer together again and eventually one passes the other. When the satellites are separated a velocity is applied to satellite B and another in the opposite direction to satellite A. In practice this means that satellite B is moved into a higher orbit and satellite A into a lower one. This causes satellite B to eventually lose speed and satellite A to gain speed. For this reason, when $A_A = 0.015\,\mathrm{m}^2$

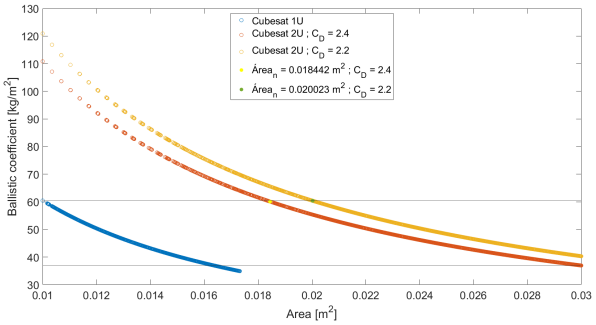

Figure 3: Coeficiente balístico de acordo com todas as áreas projetadas possíveis para dois CubeSats 1U e 2U. A $\mathrm{Área_n}$ representa a área so satélite A para o qual os coeficientes balísticos de igualam.

(in the figure 4) the satellites move apart at first but then, because the difference is small, the acceleration caused by aerodynamic resistance overlaps and they move closer together again.

When the opposite happens the acceleration of drag is greater on satellite A, in addition to speed and mass, so they move apart. These three situations are presented in figure 4.

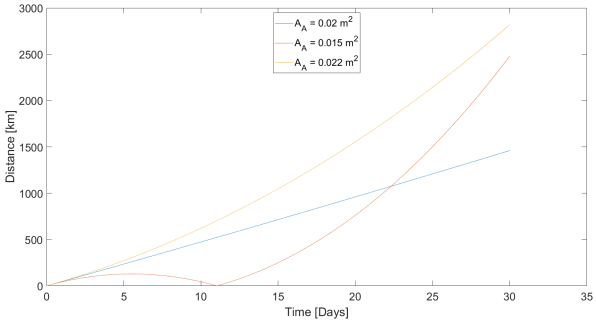

Figure 4: Relative distance between the two satellites for different values of projected area of satellite A. The simulation was performed with GMAT for 30 days, with a constant projected area value of satellite A equal to that indicated in the legend of the graph. The drag coefficient was assumed to be $C_D = 2.2$ and separation velocity $v_S = 12\,\mathrm{cm\,s^{-1}}$.

Taking into account all the considerations presented, a distance to be kept between the satellites of approximately 100 km was chosen. This choice was based on the values found in the literature and presented in the previous section. To keep the distance between the satellites a very simple control was applied based on the change of the projected area of satellite A.

When the distance from 100 km decreases, the area of satellite A is increased to about 10 % (which corresponds to a yaw angle of approximately 51° or 76°) of the $\mathrm{Area_n}$. When the distance increases the area reduces 25 % (approximately $\psi = 14°$) of the

Area_n.

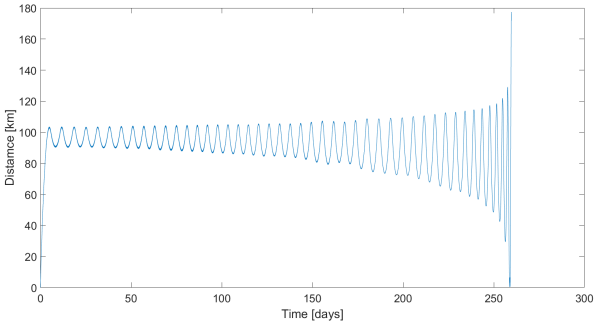

Figure 5: Distance between satellites over their lifetime.

As the altitude of the satellites decreases the aerodynamic drag increases and for this reason the maximum and minimum distance between the satellites tends to increase, as shown in figure 5.

3.3. Visibility analysis

This analysis aims to estimate the visibility of the satellite and the duration of the communication with the ground station located in Tagus Park, Lisbon. The elevation angle is the angle between the satellite and the observer's local horizon, in this case the ground station. In order to take into account possible obstacles located in the ground station area, 10° was considered as the minimum elevation angle. In figure 6 the duration of contact with the ground station for satellite A during its lifetime is shown. The contact time decreases over time, a result of the decrease in the satellite's altitude.

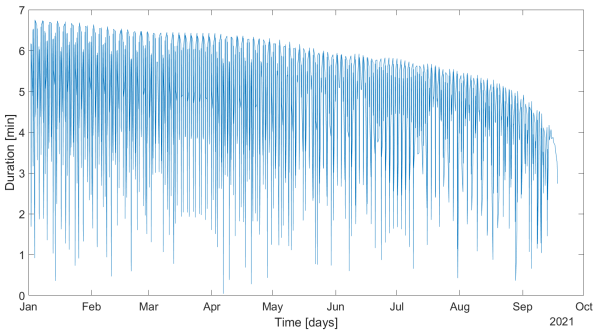

Figure 6: Visibility time over the lifetime of satellite A. The graph represents the duration of communication periods with the ground station for a minimum elevation angle of 10 degree.

Since the satellites follow approximately the same orbit behind each other, the number of contacts and the duration is approximately the same. In table 1 the important values of the contact with the ground station are shown. According to these values the satellite has on average approximately 20 min per day for communications, however some of these passages are during the eclipse phase and so in this case data transmission is to be avoided as a matter of power budget.

	Satellite A		
	Duration [min]	Contacts per day	Contacts in eclipse
Min.	0.0424	1	
Máx.	6.7530	7	
Mean	4.5489	4.6	1.5

Table 1: Satellite A contacts with ground station at TagusPark with 10° elevation. Contact duration for satellite B are approximately equal.

3.4. Eclipse time analysis

Eclipse duration throughout the mission is a very important parameter, especially for calculating the power budget since during these periods there are no power production. For low earth orbits this becomes even more important since the ratio between sunlit and eclipse time decreases with altitude.

Figure 7 shows the periods when satellite A is in eclipse and the duration of these.

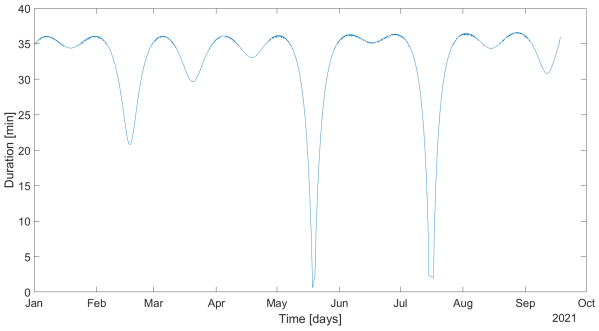

Figure 7: Eclipse time over the lifetime of satellite A.

The data for the graph was obtained by simulation with GMAT and minimum, mean and maximum values are presented in table 2.

	Min.	Mean	Max.
Eclipse duration [s]	36.3239	1982.1229	2196.4046

Table 2: Minimum, mean and maximum eclipse duration for satellite A.

Eclipse duration is directly related to the angle between the satellite's orbital plane and the Sun vector. This angle is called the beta angle and varies between −90° and 90°. When the angle has extreme values, the orbital plane is perpendicular to

the vector between the Sun and the Earth. When this happens there is no eclipse, the satellite is permanently exposed to sunlight. Figure 8 shows the value of this angle over the lifetime of the satellite. Two important factors contribute to the variation of this angle. One is the fact that the Earth is orbiting the Sun changing the direction between the Sun and the orbital plane of the satellite throughout the orbit, the other is the effect caused by the oblateness of the Earth. This effect can be seen as if the planet has more mass in the equatorial area, which slightly changes the direction of the applied gravitational force and causes nodal precession.

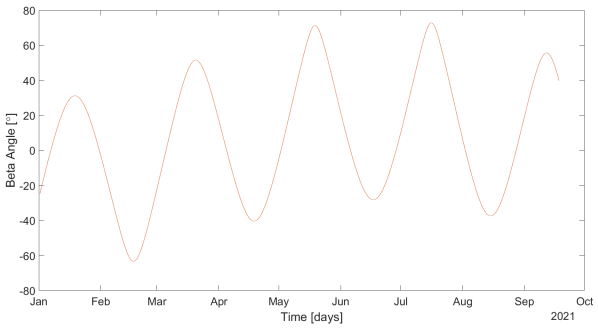

Figure 8: Sun beta angle variation throughout the mission.

It can be seen from figures 7 and 8 that the shortest eclipse times throughout the mission (between May and June and between July and August) occur when the Beta angle has a value of approximately 70°, the largest over the same time period.

3.5. Lifetime analysis

The satellite lifetime is determined from the moment the satellite is placed in orbit until it re-enters the atmosphere. As already discussed, aerodynamic drag is the largest disturbance applied to the satellite and therefore the main contributor to its lifetime. Related directly to aerodynamic drag is the drag area of the satellite which is used in this case to control the distance between the satellites. The figure 9 shows the altitude over the lifetime of the two satellites, which as we can see is practically the same even with the differences in mass and the variations in the projected area. The simulation was performed in GMAT with JacchiaRoberts as the atmospheric model.

Lifetime is always an important characteristic in a space mission. In order to prevent space debris and the number of non-functional satellites in orbit it is recommended that satellites in LEO re-enter the atmosphere before the 25 year mission [11]. This value is quite far from the value obtained for the mission, which as can be seen from the figure 9 is approximately 260 days.

In figure 10 the difference between the lifetime of

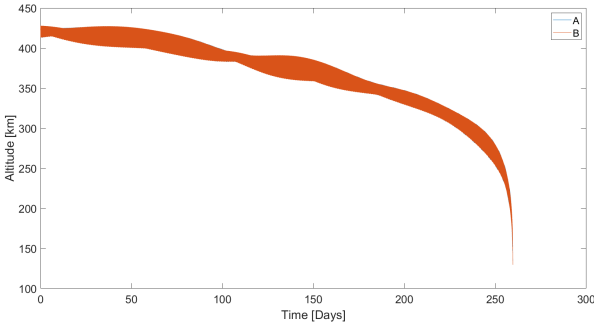

Figure 9: Satellite lifetime using GMAT and taking into account distance control (drag area change) and separation velocity. The line for satellite A is not visible because is overlapped.

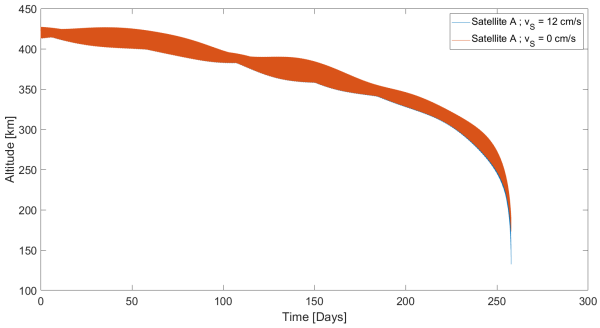

Figure 10: Effect of separation velocity on the lifetime of satellite A. Simulation made using GMAT considering a projected area of $0.02\,\mathrm{m}^2$.

satellite A with and without the separation velocity is shown. Although small it is possible to see a difference in the decay time, the satellite with $v_S = 12\,\mathrm{cm\,s^{-1}}$ has a shorter lifetime. This is due to the fact that the speed applied means a move to a lower orbit, as already mentioned.

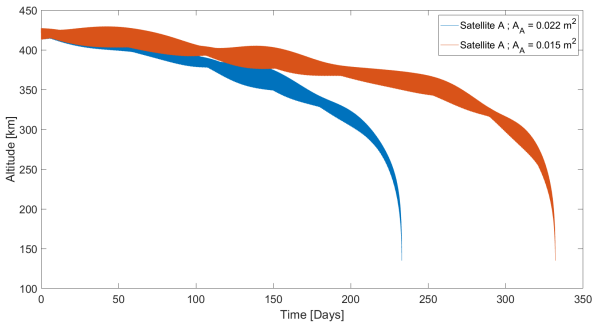

Figure 11: Effect of the limits used for the projected area on the lifetime of satellite A. When $A_A = 0.022\,\mathrm{m}^2$ the satellite decays in 233 days. When $A_A = 0.015\,\mathrm{m}^2$ the satellite decays in 332 days.

Figure 11 shows the lifetime of satellite A for two

different values of projected area but constant over time (without rotation). During the proposed mission (with rotation) the lifetime of satellite A (figure 9) lies between the two values shown but closer to the case for $A_A = 0.022\,\mathrm{m}^2$, this is because the satellite assumes this value for longer. It is possible to verify this situation in figure 5 by the duration of the valleys on the graph line, during these periods satellite A assumes a projected area of $0.022\,\mathrm{m}^2$.

4. Mission configuration

After defining the mission objectives and a preliminary analysis of the orbit, it is necessary to define the equipment to be integrated in the satellite. In this chapter a preliminary design is made using the CNES software, IDM-CIC. COTS equipment were chosen, however as in the case of ISTsat-1 it is possible to develop some products or parts to reduce the costs of the mission. Lastly, an analysis of the power, link and mass budget of the satellite is performed.

4.1. Preliminary design

In this section the preliminary design of the satellite performed with the CNES software, IDM-CIC, is presented. The positioning of the subsystems is not definitive and can be changed during the development phase, with the exception of some constraints between components. For example, the GNSS antenna must point in the direction of higher orbits where the GPS satellites are located. The star sensor of the attitude control system should also point towards zenith. Conversely, the S-band antenna and payload should be placed in the nadir direction for communication with the ground station and for Earth observation, respectively.

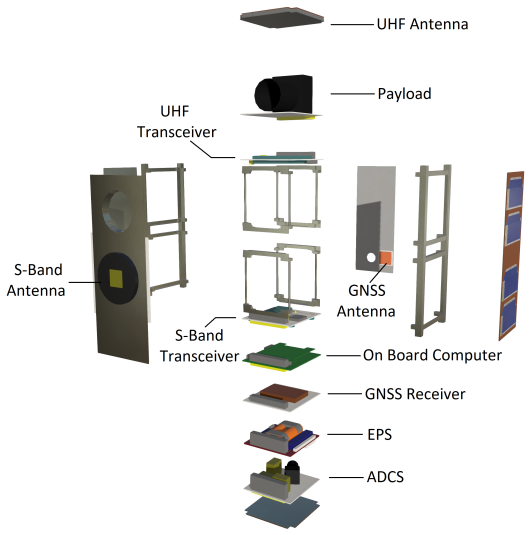

Figure 12: Exploded view of satellite A with subsystem identification.

4.2. Link budget

The reliability of a communication channel is measured by the minimum signal-to-noise ratio for a given bit error rate, BER. The BER is in turn related to the type of modulation used. Signal to noise ratio is given by

$$\frac{E_b}{N_0} = \frac{P_t G_t G_r}{k T_s R L_p} \tag{3}$$

where, E_b is bit energy, N_0 is the noise spectral density, P_t is the transmit power, G_t is the transmit antenna gain, G_r is the receiver antenna gain, k is the Boltzmann constant, T_s is the noise system temperature, R is the bit rate and finally L_p represents the free space loss.

In table 3 the intersatellite link budget of the mission is presented. Communication is done on UHF band with a frequency of 437 MHz at a distance of 150 km.

Transmitter satellite	
Transmit power, P_t [dBm]	27
Line losses, P_l [dB]	1
Antenna gain, G_t [dBi]	0
Link parameters	
Propagation path loss [dB]	-128.78
Other losses [dB]	2
Receiver satellite	
Antenna gain, G_t [dB]	0
Line losses , P_l [dB]	1
Noise temperature, T_s [K]	500
Bit rate [bps]	9600
$\frac{E_b}{N_0}$ [dB]	26.02
$\frac{E_b}{N_0}$ for BER $= 10^{-6}$ [dB]	14
Margin [dB]	12.02

Table 3: Link budget for intersatellite link with UHF band for a 150 km distance.

.

Communication with ground station is done in S-band at a frequency of 2.25 GHz. For the downlink to the ground station a parabolic antenna with diameter 2 m and a gain of 31.2 dBi was considered. For the uplink, a Yagi antenna with a gain of 16.3 dBi was considered. The model provided by AMSAT/IARU [1] was used for the analysis. The link budget results are shown in the table 4.

The downlink margin is the most critical, but although very low it is positive. It is possible to improve this value by increasing the diameter of the ground station antenna or by decreasing the bit rate.

[1] http://www.amsatuk.me.uk/iaru/spreadsheet.htm

S-Band	Uplink	Downlink
Modulation	BPSK	QPSK
Bit rate [kbit s^{-1}]	64	500
BER	10^{-6}	10^{-6}
Margin [dB]	13	4.1

Table 4: Link budget for ground station communications.

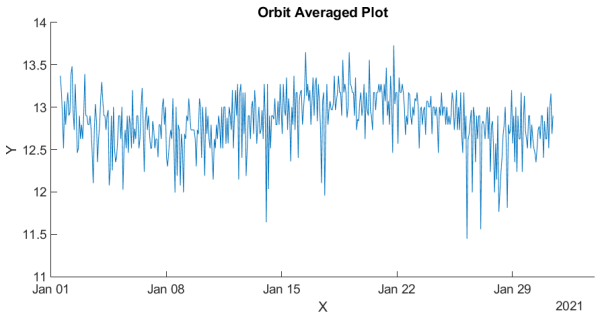

Figure 13: Orbit average power with deployable solar panels and in sun-pointing mode during 30 days. Average power is 12.8344 W.

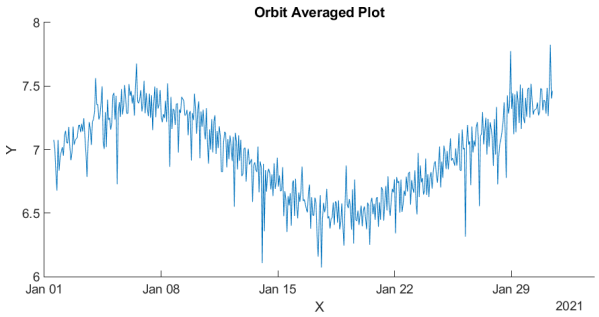

Figure 14: Orbit average power with deployable solar panels and in nadir-pointing mode during 30 days. Average power is 7.9691 W.

4.3. Power budget

In this subsection an estimate of the power produced and consumed by the satellite and consequent margin is made. First an analysis of the power consumed by the system during sunlit and eclipse phases is performed. Throughout the orbit the subsystems have different work cycles, with some only working in one or another phase and others are vital for the satellite operation and are therefore always on. The hypotheses and results considered are presented in table 5. Two different modes were evaluated during the satellite's sunlit period: sun-pointing and nadir-pointing. In the former the satellite points in the direction of the Sun to maximize energy production and storage, in the latter the satellite points in the direction of the Earth in order to fulfill the remote sensing goal and communications with ground station.

A model in MATLAB and GMAT was used [12], with some modifications, to simulate the orbit average power produced by satellite A. Two different configurations for the solar panels are considered, which directly interfere with the satellite's area of incidence. The options are scarce since the satellite has to maintain a certain position to accomplish the mission. The most obvious one is with panels mounted on the body of the satellite, the other is with deployable panels with joints on the major axis. Since the simulator does not take into account the satellite's attitude, an average constant position between the two positions assumed by the CubeSat was considered. The results are presented in figures 13 for sun-pointing mode and 14 for nadir-pointing mode.

In table 6 the most important parameters about the system power budget are presented. When the margin is negative it means that the satellite is consuming more energy than it than it produces. We can immediately conclude that configuration 1 (closed panels) does not produce enough energy for the satellite to survive. Assuming that the batteries are fully charged, the satellite in configuration 1 would only survive for 23 orbits in sun-pointing mode or 8 orbits in nadir-pointing mode. For this reason configuration 2 (open panels) is considered the final configuration. In nadir-pointing mode for configuration 2, although the margin value is small it is positive. It is possible to use the satellite only in nadir-pointing mode, however it takes approximately 160 orbits to fully charge the batteries. Whereas in sun-pointing mode only 3, but this mode implies variations of the projected area of satellite A, which would interfere with the control of the relative distance between the satellites.

4.4. Mass budget

In this section an analysis of the mass and its distribution across the satellite structure is performed. Along with the mass analysis it is also evaluated the height of the subsystems to keep the satellite within the limits of the specifications of a 2U CubeSat, the values are presented in table 7.

A 2U CubeSat should not have a mass greater than 4 kg and should not exceed 22.7 cm in height. Another important factor is the location of the center of gravity, which must be within the expected limits for this type of satellite. The limits are ±2 cm in X and Y, and ±4.5 cm in Z, relative to the geometric center of the satellite. The center of gravity is shown in table 8 for the two configurations.

5. Conclusions

This paper performs a preliminary study on the feasibility of a proposed ISTsat-2 mission, a suggestion for a second project by the ISTnanosat team.

Subsistemas	Average power [W]	Sun-pointing Duty cycle [%]	Sun-pointing Average power [W]	Nadir-pointing Duty cycle [%]	Nadir-pointing Average power [W]	Eclipse Duty de cycle [%]	Eclipse Average power [W]
ADCS	1.4	100	1.4	100	1.4	100	1.4
PAY							
Imaging	2.6	0	0	35	0.91	0	0
Readout	4	0	0	10	0.4	0	0
COM							
UHF Tx	3.5	13	0.455	13	0.455	0	0
UHF Rx	0.2	13	0.026	13	0.026	0	0
S-band Tx	5	13	0.65	13	0.65	0	0
S-band Rx	0.65	13	0.085	13	0.085	13	0.085
EPS	0.09	100	0.09	100	0.09	100	0.09
OBC	0.4	100	0.4	100	0.4	100	0.4
GNSS							
Antenna	0.03	100	0.03	100	0.03	100	0.03
Receiver	0.1	100	0.1	100	0.1	100	0.1
Total [W]			3.24		4.55		2.1045
Margin [%]			20		20		20
Total with margin [W]			3.88		5.45		2.525

Table 5: Power consumption by all subsystems during different mission modes.

Power budget	Configuration 2		Configuration 1	
	Sun-poining	Nadir-pointing	Sun-pointing	Nadir-pointing
Consumed energy during sunlit [W h]	3.8693	5.4359	3.8693	5.4359
Consumed energy during eclipse [W h]	1.3905	1.3905	1.3905	1.3905
Consumed energy / orbit [W h]	5.2598	6.8264	5.2598	6.8264
Energy generated / orbit [W h]	12.8344	6.9673	4.2834	4.0963
Margin / orbit [W h]	7.5746	0.1409	-0.9764	-3.8728
Orbits to fully charge the batteries	2.9704	159.6752	-	-
Orbits until battery discharge without energy generation	4.2778	3.2960	-	-
Orbits until battery discharge with energy generation	-	-	23.0446	8.2415

Table 6: Power budget for both configurations and in different attitude modes.

At the beginning of the mission two CubeSats are launched together in the ISS orbit and separated with a speed of $12\,\mathrm{cm\,s^{-1}}$, continuously moving apart. To counteract this, a simple control was applied using the difference between ballistic coefficient of the two CubeSats. This difference is produced by varying the drag area of satellite A depending on the intended distance for the satellites. A distance to be maintained of approximately 100 km is determined, concluding that it is possible to decrease this distance by also decreasing the separation velocity.

The earth observation system for ship detection is limited to the spatial resolution of the payload, which in this case is 16 m. It is possible to use the images for other purposes such as agriculture, atmospheric observations and ocean studies.

It was determined from the power budget that the 2U satellite in its original form does not produce enough energy to power all the subsystems. For this reason, it was decided to use deployable solar panels, and it is possible but not necessary to assume a sun-pointing mode to maximize energy production. However, using this mode interferes with the control

Subsystem	Mass [g]	Z [cm]
ADCS	400	3.1
PAY	500	6.5
COM		
UHF Antenna	89	0.6
UHF Transceiver	43	1.3
S-band Antenna	132	-
S-band Transceiver	191	1.7
EPS	184	2.65
OBC	100	1.24
GNSS		
Antenna	12	-
Receiver	25	0.75
Solar panels	350	-
Structure	390	-
Total	2416	17.84
Margin [%]	20	20
Total with margin	2899	19.62

Table 7: Mass budget and susbsystems height.

Configuration	X [cm]	Y [cm]	Z [cm]
Closed panels	0.01964	-0.03083	10.3465
Open panels	0.01817	0.3177	10.3465

Table 8: Center of gravity for both configurations with mass margins.

of the relative distance between the satellites.

All links (with ground station and intersatellite) have positive margin, however it is possible to improve the system with, for example, a larger antenna at the ground station.

The separation mechanism needs a more complete study as it is a complex element. It is important that a separation speed is imposed to avoid collisions. However it must be balanced so as not to cause rotation of the satellites. The main challenge of the mechanism is to be robust enough to survive all the challenges of launch.

Finally, is concluded that the proposed mission is theoretically possible, but poses several challenges to the team. The satellites have very complex aspects that add a degree of risk to the system. In the future, it is necessary to conduct studies dedicated to each subsystem, in particular the most critical ones, like the separation mechanism and the detachable panels wich are essential to accomplish the mission as planned.

References

[1] H. Helvajian and S. W. Janson. *Small satellites: past, present, and future*. The Aerospace Press, 2008. ISBN 978-1-884989-22-3. doi:10.2514/4.989223.

[2] B. Lal, E. de la Rosa Blanco, J. R. Behrens, B. A. Corbin, E. Green, A. J. Picard, and A. Balakrishnan. *Global trends in small satellites*, 2017.

[3] G. P. Newton, R. Horowitz, and W. Priester. Atmospheric density and temperature variations from the explorer xvii satellite and a further comparison with satellite drag. *Planetary and Space Science*, 13(7):599–616, 1965. ISSN 0032-0633. doi:10.1016/0032-0633(65)90042-5.

[4] C. L. Leonard. *Formationkeeping of spacecraft via differential drag*. PhD thesis, Massachusetts Institute of Technology, July 1986.

[5] R. Bevilacqua and M. Romano. Rendezvous maneuvers of multiple spacecraft using differential drag under j2 perturbation. *Journal of Guidance, Control, and Dynamics*, 31(6): 1595–1607, 2008. doi:10.2514/1.36362.

[6] T. Finley, D. Rose, K. Nave, W. Wells, J. Redfern, R. Rose, and C. Ruf. Techniques for leo constellation deployment and phasing utilizing differential aerodynamic drag. *Advances in the Astronautical Sciences*, 150:1397–1411, 01 2014.

[7] A Direção-Geral de Recursos Naturais, Segurança e Serviços Marítimos . Sistema costeiro de vts, 2020. URL `https://www.dgrm.mm.gov.pt/pt/web/guest/sistema-costeiro-de-vts`. Acedido a 21-06-2020.

[8] R. Radhakrishnan, W. W. Edmonson, F. Afghah, R. M. Rodriguez-Osorio, F. Pinto, and S. C. Burleigh. Survey of inter-satellite communication for small satellite systems: Physical layer to network layer view. *IEEE Communications Surveys & Tutorials*, 18(4):2442–2473, 2016. doi:10.1109/COMST.2016.2564990.

[9] A. Budianu, T. J. W. Castro, A. Meijerink, and M. J. Bentum. Inter-satellite links for cubesats. In *2013 IEEE Aerospace Conference*, pages 1–10, 2013. doi:10.1109/AERO.2013.6496947.

[10] Y. F. Wong, O. Kegege, S. Schaire, G. M. Bussey, S. Altunç, Y. Zhang, and C. Patel. An optimum space-to-ground communication concept for cubesat platform utilizing nasa space network and near earth network. *30th Annual AIAA/USU Conference on Small Satellites*, 2016.

[11] IADC Steering Group. Space debris mitigation guidelines. Technical Report 5, Inter-Agency Space Debris Coordination Committee, May 2020.

[12] T. Etchells and L. Berthoud. Developing a power modelling tool for cubesats. *33rd Annual AIAA/USU Conference on Small Satellites*, 2019.